Organic LETTERS

Letter

pubs.acs.org/OrgLett

Starburst Triarylamine Donor-Based Metal-Free Photosensitizers for Photocatalytic Hydrogen Production from Water

Po-Yu Ho,[†,‡,∥] Yi Wang,[†,∥] Sze-Chun Yiu,[†] Wai-Hong Yu,[†] Cheuk-Lam Ho,*[,†,‡] and Shuping Huang*[,§]

[†]Institute of Molecular Functional Materials, Department of Chemistry and Institute of Advanced Materials, Hong Kong Baptist University, Waterloo Road, Kowloon Tong, Hong Kong, P. R. China

[‡]HKBU Institute of Research and Continuing Education, Shenzhen Virtual University Park, Shenzhen, 518057, P. R. China

[§]College of Chemistry, Fuzhou University, Fuzhou, Fujian 350108, P. R. China

Supporting Information

ABSTRACT: Three metal-free molecular photosensitizers (**S1**−**S3**) featuring a starburst triarylamine donor moiety have been synthesized. They show attractive photocatalytic performance in visible light-driven H_2 production from water in their platinized TiO_2 composites. A remarkable H_2 turnover number (TON) of 10 200 (48 h) was achieved in an **S1**-anchored system.

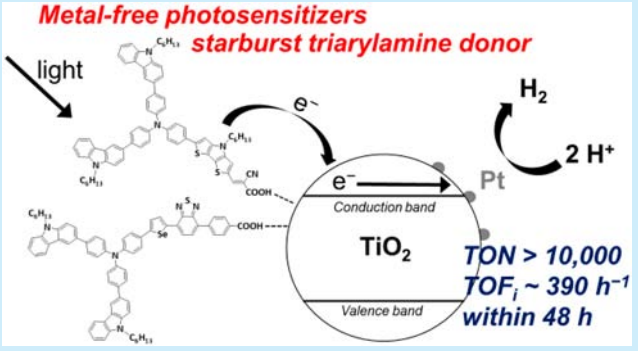

In the field of solar-fuel production, photocatalytic water splitting reaction,[1] which converts water molecules (feedstock) into hydrogen (fuel) and oxygen molecules through a light-driven photocatalytic process, has been regarded as a primary research direction. In essence, the water splitting reaction could be comprehended in terms of two redox half-reactions: the cathodic half-reaction refers to the reduction of two aqueous protons to one H_2 molecule, and the anodic half-reaction corresponds to the oxidation of two H_2O molecules to one O_2 molecule.[2] Importantly, these two half-reactions could be independently investigated for their mechanisms and then be recombined together to examine the overall H_2 productiveness.[3]

For the cathodic side, a feasible system should consist of a photosensitizer (PS) for exciton formation, a pathway for charge separation,[4] a catalyst for H_2 production through a catalytic cycle upon electron collection, aqueous protons, and a sacrificial electron donor (SED) as an electron source.[5] Under such a setting, many different systems have been developed over the past three decades while platinized TiO_2 and colloidal platinum are the two most well-known and common photocatalysts because of their excellent performances in catalytic reactions.[6]

As visible light PSs, metalated dyes have been extensively investigated for water reduction.[5] In order to reduce the total noble metal content in the photocatalytic system, we revisited the library of organic dyes and looked for suitable candidates to act as molecular PSs. However, metal-free PSs for photocatalytic H_2 generation are sparsely reported in the literature and most suffer from instability (only active within 10 h) and/or poor activity (TOF < 100 h^{-1}).[7]

Herein, three metal-free PSs (**S1**−**S3**) were synthesized with either a donor−π−acceptor (D−π−A)[8] or donor−acceptor−π−acceptor′ (D−A−π−A′) framework,[9] in particular with the same starburst triarylamine donor moiety (D) (Figure 1).[10] These molecules match well with the prerequisites of PSs in both photocatalytic H_2 generation and dye-sensitized solar cells (DSSCs), and the corresponding studies have been carried out.

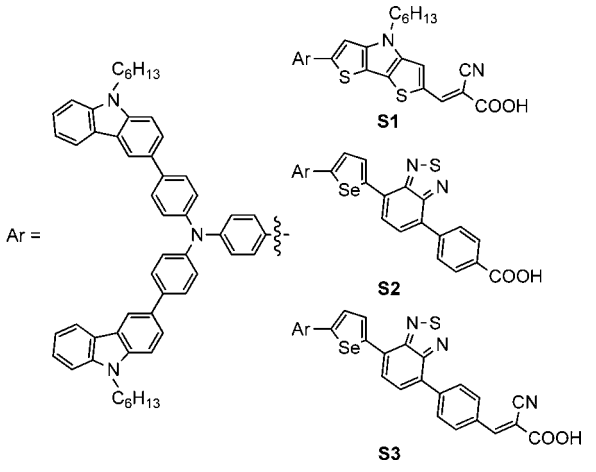

Figure 1. Chemical structures of photosensitizers **S1**−**S3**.

Received: January 6, 2017
Published: February 10, 2017

DOI: 10.1021/acs.orglett.7b00042
Org. Lett. 2017, 19, 1048−1051

The synthetic routes for **S1**−**S3** are shown in Schemes 1 and S1 (in the Supporting Information, SI). The precursors **7a**−**7c**

Scheme 1. Synthetic Routes for S1−**S3**

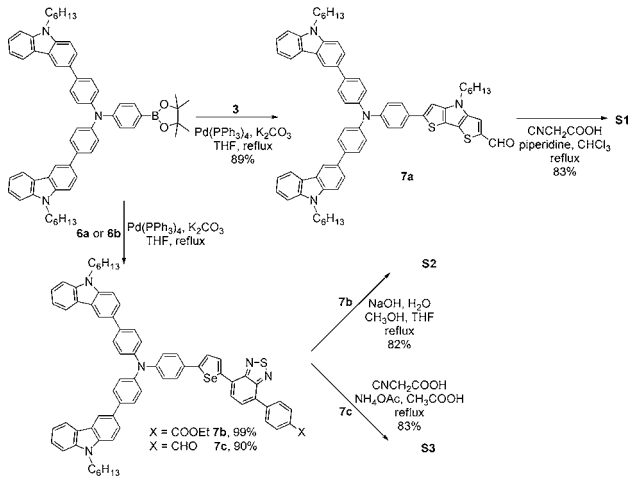

were prepared by Suzuki coupling reaction of the corresponding intermediates with the arylboronic ester, in which the aryl group is the starburst triarylamine unit.[10] Eventually, two different Knoevenagel condensation approaches were launched to prepare **S1** and **S3** by using cyanoacetic acid, while **S2** was obtained through the deprotection of the ethyl group in **7b** under basic conditions. All of the target PSs are air-stable and have been fully characterized by matrix-assisted laser desorption ionization time-of-flight (MALDI-TOF) mass spectrometry, and ^{1}H and ^{13}C NMR spectroscopy (Figures S1−S26, SI).

The UV/vis absorption and emission spectra of **S1**−**S3** measured in dichloromethane solution are shown in Figure 2,

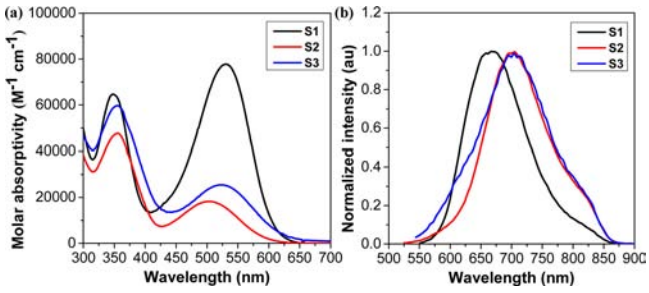

Figure 2. (a) UV/vis absorption spectra and (b) normalized photoluminescence spectra of **S1**−**S3** in CH_2Cl_2 at 293 K (excited at the ICT absorption peaks, respectively).

and the corresponding data are listed in Table 1. All the organic dyes display two broad distinct absorption bands in the range of 300−650 nm. The absorption bands in the short wavelength region (centered at 347−356 nm) are allocated to the localized π−π* transitions among aromatic rings, while those in the longer wavelength region (centered at 503−531 nm) are attributed to the intramolecular charge transfer (ICT) from an electron-rich moiety to an electron-deficient group. The peak absorption wavelengths of ICT bands are blue-shifted in the order of **S1** (531 nm) > **S3** (523 nm) > **S2** (503 nm). This is correlated to the different electron-withdrawing abilities of electron acceptors (A and A′) and different electron-donating strengths of the π-linkers. Density functional theory (DFT) calculation was performed for **S1**−**S3**; the electron density in HOMO is associated with the donor moiety and the π-linker, while the LUMO is localized at the electron acceptor (Figures S27−S31 and Tables S1−S2, SI). Thus, it is further confirmed the photoexcitation can induce ICT from the starburst donor moiety and π-linker to cyanoacetate or acid groups. On the other hand, these three PSs show photoluminescence in CH_2Cl_2 at ambient temperature. They exhibit solely one broad and structureless emission peak with maxima at 667, 704, and 704 nm with emission lifetimes of 2.0, 2.2, and 2.1 ns for **S1**−**S3**, respectively. No emission band is observed from the triplet excited state over the measured spectral window. Both emission pattern and lifetime regime are suggestive to their fluorescent nature.[11]

Table 1. Absorption and Emission Data of S1−**S3 in CH_2Cl_2**

dye	λ_{abs} (ε /M^{-1} cm^{-1})/nm	λ_{onset}/nm	λ_{em}/nm	τ_f/ns
S1	347 (64 680), 531 (77 760)	608	667	2.0
S2	355 (59 777), 503 (18 272)	596	704	2.2
S3	356 (47 528), 523 (25 449)	630	704	2.1

Cyclic voltammetry (CV) measurements focusing on positive applied potential was performed. The recorded cyclic voltammograms are illustrated in Figures S32 and S33 (SI), and the obtained data are summarized in Table S3 (SI). It was found that the E_{HOMO} of these dyes (ranging from −5.01 to −5.13 eV) are more negative than the redox potential energy levels of ascorbic acid (AA)[12] (−4.65 eV, pH ≈ 4) and I^-/I_3^- redox couple[13] (∼ −4.9 eV). This assures dye regeneration of the oxidized dyes takes place rapidly in both photocatalytic and DSSCs systems.[14] Meanwhile, the E_{LUMO} of these dyes (ranging from −2.98 to −3.05 eV) are much more positive than the conduction band energy level of TiO_2 (∼ −4.0 eV); therefore, a swift electron injection process is anticipated to occur.[15]

The photovoltaic properties of **S1**−**S3** were preliminarily investigated by fabricating conventional DSSC devices (Experimental section, SI). The relevant device performance parameters are tabulated in Table S4. Figure S34 displays the photocurrent density−voltage curves (J−V curves) and incident-photon-to-current conversion efficiency (IPCE) spectra. The highest power conversion efficiency (PCE) of 6.59% (short-circuit current density (J_{sc}) = 14.23 mA cm^{-2}, open-circuit voltage (V_{oc}) = 0.68 V, and fill factor (FF) = 0.679) was obtained with **S1**, while **S2** and **S3** rendered PCEs of 6.21% and 5.55%, respectively. In particular, **S1** with the dithienopyrrole fused aromatic ring as the π-linker displays the largest J_{sc} value as compared to that of auxiliary acceptor-containing **S2** and **S3**, indicating that this exceptionally strong electron-donating π-linker[16] is effective to strengthen and broaden its light absorption and raise the J_{sc}. As a result, the maximum IPCE value achieved by **S1** is larger than 70% at ∼500 nm. Furthermore, the corresponding Nyquist plots (Figure S35, SI) from electrochemical impedance spectroscopy (EIS, dark condition) disclose the resistance of electron recombination (R_{rec}) at the interfaces between the TiO_2, PS, and redox electrolytes (Table S4).[17] It was found that these PSs exhibited very similar R_{rec} values, and thus similar V_{oc} values from their J−V curves were accounted. This circumstance is best explained by the dominant influences brought from the same starburst triarylamine donor moiety in **S1**−**S3** since this functional group was proven to be valid in

DOI: 10.1021/acs.orglett.7b00042
Org. Lett. 2017, 19, 1048−1051

inhibiting dye aggregation and charge recombination at the interfaces due to its bulky and hydrophobic nature.[10]

In view of the superior light-harvesting capability in the 450−600 nm region for **S1**−**S3**, we anticipate **S1**−**S3** could be utilized to examine the promotion of photocatalytic H_2 production from water. In this aspect, Eisenberg and co-workers recently reported that some platinum-containing dyads as the PSs enabled unprecedentedly efficient and steady H_2 production from water after attaching to platinized TiO_2 nanoparticles.[18] Herein, we carried out the light-driven H_2 generation studies by adapting the same photocatalytic system on our organic PSs. Detailed procedures could be referred to in the Experimental section and Figures S36−S38 (SI).

H_2 generation fitting curves (vs time) for **S1**−**S3** are illustrated in Figure 3, and the corresponding data (TON, TOF, TOF_i, $Activity_i$, and AQY_i%) are tabulated in Table 2. PSs **S1**−**S3** potently facilitated the photocatalytic H_2 generation (>18 mL over 48 h) while the system without PS (as a control) only produced less than 1 mL of H_2 and the system with **Eosin Y** (as a standard dye[19]) generated ∼1 mL of H_2. The system with **S1** afforded the highest photocatalytic activity with a TON of 10 200 over 48 h, while the systems with **S2** and **S3** also attained TONs of 9520 and 6260, respectively, in the same duration. In order to obtain a reasonable comparison with other photocatalytic systems reported in the literature, the initial H_2 generation activity ($Activity_i$) and initial apparent quantum yield (AQY_i) for each PS were also reported. Notably, the most active system with **S1** attained a high $Activity_i$ of 478 000 μmol g^{-1} h^{-1} with a decent AQY_i of ∼12%. To the best of our knowledge, the system with **S1** is indeed one of the most efficient and robust photocatalytic H_2 generation systems adopting TiO_2-anchoring molecular PS in the literature, according to the TOF and TON values. When **S1** is compared with **S2** and **S3**, the better performance of **S1** is ascribed to the more intense absorption profile in 400−600 nm. In addition, by comparing the photocatalytic reaction mixture of **S1** before and after the irradiation (48 h) (Figure S40, SI), the TiO_2 composite material still remained the original color and the AA aqueous solution changed from colorless to pale yellow due to the presence of dehydroascorbic acid (DHA) resulting from the dye-regeneration reaction. This indicated that issues regarding dye desorption[20] and photobleaching of PS were not observed in our case.[18b] In combination with the H_2 generation curve, it is reasonable to expect the photocatalytic system with **S1** is still highly active even under a longer duration of illumination.

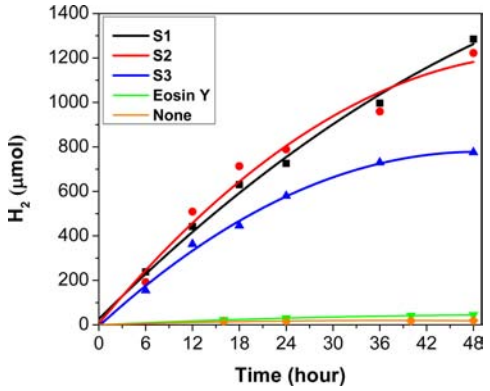

Figure 3. Kinetic traces of H_2 generation with respect to different photosensitizers (**S1**−**S3** and **Eosin Y**) under radiation of green LED (520 nm) at 50 mW. Each sample consisted of 5 mL of 0.5 M ascorbic acid in water at pH 4.0 to which 20 mg of PS-TiO_2-Pt composite material was added.

In comparison with those noble metal-containing complexes (e.g., Ru(II),[21] Ir(III),[22] and Pt(II) complexes[18b,23]) with outstanding photocatalytic performance (Table S5, SI), PSs **S1**−**S3** obviously lack 'heavy' metals or atoms. These PSs were supposed to mainly utilize their singlet excited state but not triplet state for the electron transfer. Theoretically, the atom with the largest atomic number in their chemical structures is sulfur (Z = 16, **S1**) or selenium (Z = 34, **S2** and **S3**), while the atomic numbers of these two elements are still considerably smaller than those of ruthenium (Z = 44), iridium (Z = 77), and platinum (Z = 78), so ineffective intersystem crossing (ISC) is likely to be present. Therefore, there should be a significant but hidden factor(s) leading to the distinctive efficiency and longevity of **S1**.

Most of the reported metalated[24] and metal-free PSs[25] are found to be unstable upon light irradiation in the photocatalytic system. This is mainly attributed to the formation of reduced species of PS (i.e., PS^-) which comes from the reductive quenching pathway.[5] This species would undergo decomposition easily during the photocatalytic process. Therefore, the improvement of photocatalytic performance can be realized if the excited species PS* is *unfavorably* reduced by the SED. Thus, the electron-rich and hydrophobic starburst donor moiety in **S1**−**S3** is envisaged to function like a shield to combat against the formation of PS^- after anchoring onto platinized TiO_2 nanoparticles. Previous studies from other groups support our idea in unveiling the relationship among bulky substituents on the PS, rate of reductive quenching, and H_2 production activity.[26] Moreover, the starburst donor moiety design has also been suggested to increase the dye regeneration rate in DSSCs due to the larger surface area occupied by the donor moiety.[27] Hence, the retardation against the decomposition of metastable oxidized species PS^+ is accomplished simultaneously.[28] Similar effects in the case of H_2 production are most likely attained as well, so **S1**−

Table 2. Light-Driven H_2 Generation Data with and without Photosensitizers S1−S3 and Eosin Y

dye	DL%[a]	H_2 (mL)	TON[b]	TOF[c] (h^{-1})	TOF_i[d] (h^{-1})	$Activity_i$[e] (μmol g^{-1} h^{-1})	AQY_i%[f]
S1	99	30.3	10 200	213	385	478 000	12.3
S2	99	28.3	9520	198	360	446 000	11.5
S3	99	18.6	6260	130	232	288 000	7.44
Eosin Y	100	1.06	354	7.4	12	15 000	0.35
none	–	0.45	–	–	–	10 400	0.23

[a]Dye-loading percentage. [b]Turnover number of H_2 is calculated as number of mole of H_2 produced divided by the number of mole of PS attached to platinized TiO_2. [c]Turnover frequency is calculated per hour. [d]Initial turnover frequency in the first 2 h. [e]Initial photocatalytic activity of the system is defined as number of micromole of H_2 evolved per gram of platinum loaded per hour. [f]Initial apparent quantum yield percentage (AQY_i%) of the system.

DOI: 10.1021/acs.orglett.7b00042
Org. Lett. 2017, 19, 1048−1051

S3 should be more stable as compared to other PSs without the starburst donor moiety (performance shown in Table S6, SI).

In summary, three metal-free PSs featuring a starburst triarylamine donor moiety were synthesized and employed in the photocatalytic H_2 production from water. Specifically, **S1** attained an active and robust H_2 generation system (TOF_i of 385 h^{-1} and TON of 10 200) over 48 h. Notably, the electron-rich and hydrophobic starburst triarylamine donor design has great potential in improving the robustness of organic PSs in the photocatalytic system.

■ ASSOCIATED CONTENT

Supporting Information

The Supporting Information is available free of charge on the ACS Publications website at DOI: 10.1021/acs.orglett.7b00042.

Details of experimental procedures, synthesis and characterization data of compounds, computational studies, photovoltaic performances of DSSCs and H_2 generation studies (PDF)

■ AUTHOR INFORMATION

Corresponding Authors

*E-mail: clamho@hkbu.edu.hk.
*E-mail: huangshp@gmail.com.

ORCID

Cheuk-Lam Ho: 0000-0001-8596-0307

Author Contributions

‖P.-Y.H. and Y.W. contributed equally to this work.

Notes

The authors declare no competing financial interest.

■ ACKNOWLEDGMENTS

C.-L.H. thanks Hong Kong Baptist University (FRG2/15-16/074 and FRG1/15-16/043), the National Natural Science Foundation of China (Project No. 21504074), and the Science, Technology and Innovation Committee of Shenzhen Municipality (JCYJ20160531193836532) for their financial support.

■ REFERENCES

(1) Hisatomi, T.; Kubota, J.; Domen, K. *Chem. Soc. Rev.* **2014**, *43*, 7520−7535.
(2) Bard, A. J.; Fox, M. A. *Acc. Chem. Res.* **1995**, *28*, 141−145.
(3) Maeda, K.; Domen, K. *J. Phys. Chem. Lett.* **2010**, *1*, 2655−2661.
(4) (a) Han, W.-S.; Wee, K.-R.; Kim, H.-Y.; Pac, C.; Nabetani, Y.; Yamamoto, D.; Shimada, T.; Inoue, H.; Choi, H.; Cho, K.; Kang, S. O. *Chem. - Eur. J.* **2012**, *18*, 15368−15381. (b) Brennaman, M. K.; Dillon, R. J.; Alibabaei, L.; Gish, M. K.; Dares, C. J.; Ashford, D. L.; House, R. L.; Meyer, G. J.; Papanikolas, J. M.; Meyer, T. J. *J. Am. Chem. Soc.* **2016**, *138*, 13085−13102.
(5) Eckenhoff, W. T.; Eisenberg, R. *Dalton Trans.* **2012**, *41*, 13004−13021.
(6) Kemppainen, E.; Bodin, A.; Sebok, B.; Pedersen, T.; Seger, B.; Mei, B.; Bae, D.; Vesborg, P. C. K.; Halme, J.; Hansen, O.; Lund, P. D.; Chorkendorff, I. *Energy Environ. Sci.* **2015**, *8*, 2991−2999.
(7) Cecconi, B.; Manfredi, N.; Montini, T.; Fornasiero, P.; Abbotto, A. *Eur. J. Org. Chem.* **2016**, *2016*, 5194−5215.
(8) Wang, Z.-S.; Koumura, N.; Cui, Y.; Takahashi, M.; Sekiguchi, H.; Mori, A.; Kubo, T.; Furube, A.; Hara, K. *Chem. Mater.* **2008**, *20*, 3993−4003.
(9) Zhu, W.; Wu, Y.; Wang, S.; Li, W.; Li, X.; Chen, J.; Wang, Z.-s.; Tian, H. *Adv. Funct. Mater.* **2011**, *21*, 756−763.
(10) Ho, P.-Y.; Siu, C.-H.; Yu, W.-H.; Zhou, P.; Chen, T.; Ho, C.-L.; Lee, L. T. L.; Feng, Y.-H.; Liu, J.; Han, K.; Lo, Y. H.; Wong, W.-Y. *J. Mater. Chem. C* **2016**, *4*, 713−726.
(11) Wong, W.-Y.; Wang, X.-Z.; He, Z.; Chan, K.-K.; Djurišić, A. B.; Cheung, K.-Y.; Yip, C.-T.; Ng, A. M.-C.; Xi, Y. Y.; Mak, C. S. K.; Chan, W.-K. *J. Am. Chem. Soc.* **2007**, *129*, 14372−14380.
(12) Li, X.; Yu, J.; Low, J.; Fang, Y.; Xiao, J.; Chen, X. *J. Mater. Chem. A* **2015**, *3*, 2485−2534.
(13) Robson, K. C. D.; Bomben, P. G.; Berlinguette, C. P. *Dalton Trans.* **2012**, *41*, 7814−7829.
(14) Haque, S. A.; Palomares, E.; Cho, B. M.; Green, A. N. M.; Hirata, N.; Klug, D. R.; Durrant, J. R. *J. Am. Chem. Soc.* **2005**, *127*, 3456−3462.
(15) Bessho, T.; Yoneda, E.; Yum, J.-H.; Guglielmi, M.; Tavernelli, I.; Imai, H.; Rothlisberger, U.; Nazeeruddin, M. K.; Grätzel, M. *J. Am. Chem. Soc.* **2009**, *131*, 5930−5934.
(16) Polander, L. E.; Yella, A.; Teuscher, J.; Humphry-Baker, R.; Curchod, B. F. E.; Ashari Astani, N.; Gao, P.; Moser, J.-E.; Tavernelli, I.; Rothlisberger, U.; Grätzel, M.; Nazeeruddin, M. K.; Frey, J. *Chem. Mater.* **2013**, *25*, 2642−2648.
(17) Bisquert, J. *Phys. Chem. Chem. Phys.* **2003**, *5*, 5360−5364.
(18) (a) Meyer, G. J. *Proc. Natl. Acad. Sci. U. S. A.* **2015**, *112*, 9146−9147. (b) Zheng, B.; Sabatini, R. P.; Fu, W.-F.; Eum, M.-S.; Brennessel, W. W.; Wang, L.; McCamant, D. W.; Eisenberg, R. *Proc. Natl. Acad. Sci. U. S. A.* **2015**, *112*, E3987−E3996. (c) Ho, P.-Y.; Zheng, B.; Mark, D.; Wong, W.-Y.; McCamant, D. W.; Eisenberg, R. *Inorg. Chem.* **2016**, *55*, 8348−8358.
(19) (a) Li, Q.; Jin, Z.; Peng, Z.; Li, Y.; Li, S.; Lu, G. *J. Phys. Chem. C* **2007**, *111*, 8237−8241. (b) Li, Q.; Chen, L.; Lu, G. *J. Phys. Chem. C* **2007**, *111*, 11494−11499.
(20) Le, T. T.; Akhtar, M. S.; Park, D. M.; Lee, J. C.; Yang, O.-B. *Appl. Catal., B* **2012**, *111−112*, 397−401.
(21) (a) Sun, Y.; Sun, J.; Long, J. R.; Yang, P.; Chang, C. J. *Chem. Sci.* **2013**, *4*, 118−124. (b) Ott, S.; Kritikos, M.; Åkermark, B.; Sun, L. *Angew. Chem., Int. Ed.* **2003**, *42*, 3285−3288. (c) Khnayzer, R. S.; Thoi, V. S.; Nippe, M.; King, A. E.; Jurss, J. W.; El Roz, K. A.; Long, J. R.; Chang, C. J.; Castellano, F. N. *Energy Environ. Sci.* **2014**, *7*, 1477−1488.
(22) (a) Metz, S.; Bernhard, S. *Chem. Commun.* **2010**, *46*, 7551−7553. (b) DiSalle, B. F.; Bernhard, S. *J. Am. Chem. Soc.* **2011**, *133*, 11819−11821.
(23) (a) Wang, X.; Goeb, S.; Ji, Z.; Pogulaichenko, N. A.; Castellano, F. N. *Inorg. Chem.* **2011**, *50*, 705−707. (b) Du, P.; Schneider, J.; Jarosz, P.; Eisenberg, R. *J. Am. Chem. Soc.* **2006**, *128*, 7726−7727.
(24) Tinker, L. L.; McDaniel, N. D.; Curtin, P. N.; Smith, C. K.; Ireland, M. J.; Bernhard, S. *Chem. - Eur. J.* **2007**, *13*, 8726−8732.
(25) (a) Shimidzu, T.; Iyoda, T.; Koide, Y. *J. Am. Chem. Soc.* **1985**, *107*, 35−41. (b) Lazarides, T.; McCormick, T.; Du, P.; Luo, G.; Lindley, B.; Eisenberg, R. *J. Am. Chem. Soc.* **2009**, *131*, 9192−9194. (c) Zhang, P.; Wang, M.; Dong, J.; Li, X.; Wang, F.; Wu, L.; Sun, L. *J. Phys. Chem. C* **2010**, *114*, 15868−15874.
(26) (a) Lee, J.; Kwak, J.; Ko, K. C.; Park, J. H.; Ko, J. H.; Park, N.; Kim, E.; Ryu, D. H.; Ahn, T. K.; Lee, J. Y.; Son, S. U. *Chem. Commun.* **2012**, *48*, 11431−11433. (b) Deponti, E.; Natali, M. *Dalton Trans.* **2016**, *45*, 9136−9147.
(27) Zhao, L.; Wagner, P.; Barnsley, J. E.; Clarke, T. M.; Gordon, K. C.; Mori, S.; Mozer, A. J. *Chem. Sci.* **2016**, *7*, 3506−3516.
(28) (a) Li, F.; Jennings, J. R.; Wang, Q. *ACS Nano* **2013**, *7*, 8233−8242. (b) Daeneke, T.; Mozer, A. J.; Uemura, Y.; Makuta, S.; Fekete, M.; Tachibana, Y.; Koumura, N.; Bach, U.; Spiccia, L. *J. Am. Chem. Soc.* **2012**, *134*, 16925−16928.

DOI: 10.1021/acs.orglett.7b00042
Org. Lett. 2017, 19, 1048−1051